An Energy and Angular-Momentum Conserving Vertical Finite-Difference Scheme and Hybrid Vertical Coordinates

A. J. SIMMONS AND D. M. BURRIDGE

European Centre for Medium Range Weather Forecasts, Shinfield Park, Reading, Berkshire, U.K.

(Manuscript received 12 August 1980, in final form 25 November 1980)

ABSTRACT

An energy and angular-momentum conserving vertical finite-difference scheme is introduced for a general terrain-following vertical coordinate which is a function of pressure and its surface value. A corresponding semi-implicit time scheme is also defined. These schemes are used to compare the usual sigma coordinate with the hybrid coordinate which reduces to pressure above a fixed level and with a modified hybrid coordinate which tends uniformly to pressure at upper levels. Error in the representation of the stratospheric pressure gradient over steep orography can be significantly reduced by use of the hybrid coordinate, but the semi-implicit scheme is less stable. The modified hybrid coordinate offers a useful compromise.

1. Introduction

The use of sigma, pressure divided by its surface value, rather than pressure as the vertical coordinate in a primitive equation model (Phillips, 1957) produces a system of equations with a much simpler lower boundary condition, but this simplicity is obtained at the expense of introducing other difficulties. Over steep orography care has to be taken to ensure cancellation between the two components which comprise the pressure gradient in the momentum equation. Observational analysis and diagnosis are commonly carried out in pressure coordinates, and over high orography the analysis, when used to provide initial data for a sigma-coordinate model, needs to be carried out at a higher level than would be the case for a pressure coordinate model with a similar top level over the oceans. Some of these difficulties become particularly apparent in models designed largely for stratospheric simulation, and to circumvent them models have been developed with a hybrid vertical coordinate suggested by Sangster (1960) which is similar to the usual sigma coordinate at low levels, but which reduces to pressure above a certain fixed level (Schlesinger and Mintz, 1979; Fels *et al.*, 1980).

The purpose of the present paper is twofold. First, in the following three sections we set down the form of the continuous primitive equations for a general terrain-following vertical coordinate, following Kasahara (1974), and then present a vertical finite-difference formulation of these equations which conserves both energy and angular momentum. We include also a formulation of a corresponding semi-implicit time scheme. Second, we use these formulations to compare three different vertical coordinates. Two of these are the usual sigma coordinate and the hybrid coordinate which reduces to pressure above a certain level. The latter exhibits a number of advantages over the sigma coordinate, but has the disadvantage of a marked irregularity in the distribution of layer thickness over high ground. We thus also investigate a third vertical coordinate for which the transition toward a pure pressure coordinate occurs smoothly as the pressure decreases toward zero.

The different vertical coordinates are examined in two respects. We first follow a number of authors, among them Corby *et al.* (1972), Gary (1973), Sundqvist (1976) and Nakamura (1978), in examining the error in the representation of the pressure gradient over steep orography. Second, we examine the stability of the semi-implicit time scheme as analyzed for a sigma-coordinate model by Simmons *et al.* (1978).

2. The continuous formulation

We consider a general, terrain-following, vertical coordinate η, a monotonic function of pressure p and dependent on its surface value p_s:

$$\eta = h(p, p_s),$$

where $h(0, p_s) = 0$ and $h(p_s, p_s) = 1$. The continuous formulation of the primitive equations may be directly written down following Kasahara (1974).

The momentum and thermodynamic equations for frictionless adiabatic motion are

$$\frac{D\mathbf{v}}{Dt} + f\mathbf{k} \times \mathbf{v} + \nabla\phi + \frac{RT}{p}\nabla p = 0, \quad (2.1)$$

0027-0644/81/040758-09$06.25

$$\frac{DT}{Dt} - \frac{\kappa T\omega}{p} = 0. \tag{2.2}$$

The continuity equation may be written

$$\frac{\partial}{\partial\eta}\left(\frac{\partial p}{\partial t}\right) + \nabla\cdot\left(\mathbf{v}\frac{\partial p}{\partial\eta}\right) + \frac{\partial}{\partial\eta}\left(\dot{\eta}\frac{\partial p}{\partial\eta}\right) = 0, \tag{2.3}$$

while the hydrostatic equation is

$$\frac{\partial\phi}{\partial\eta} = -\frac{RT}{p}\frac{\partial p}{\partial\eta}. \tag{2.4}$$

Here t is time and D/Dt is the material derivative, which in η coordinates takes the form

$$\frac{\partial}{\partial t} + u\frac{\partial}{\partial x} + v\frac{\partial}{\partial y} + \dot{\eta}\frac{\partial}{\partial\eta}$$

for a Cartesian coordinate system with x eastward and y northward, and eastward and northward velocity components u and v. $\mathbf{v}$ is the horizontal velocity vector, $\mathbf{v} = (u, v, 0)$, and ∇ the horizontal gradient operator; $\nabla \equiv (\partial/\partial x, \partial/\partial y, 0)$ for the Cartesian system. f is the Coriolis parameter, $\mathbf{k}$ the unit vertical vector, ϕ the geopotential, T the temperature, R the gas constant and $\kappa = R/c_p$, where c_p is the specific heat at constant pressure. ω is given by

$$\omega \equiv \frac{Dp}{Dt} = -\int_0^\eta \nabla\cdot\left(\mathbf{v}\frac{\partial p}{\partial\eta}\right)d\eta + \mathbf{v}\cdot\nabla p. \tag{2.5}$$

Explicit expressions for the rate of change of surface pressure, and for $\dot{\eta}$, are obtained by integrating (2.3) using the boundary conditions $\dot{\eta} = 0$ at $\eta = 0$ and $\eta = 1$:

$$\frac{\partial p_s}{\partial t} = -\int_0^1 \nabla\cdot\left(\mathbf{v}\frac{\partial p}{\partial\eta}\right)d\eta \tag{2.6}$$

$$\dot{\eta}\frac{\partial p}{\partial\eta} = -\frac{\partial p}{\partial t} - \int_0^\eta \nabla\cdot\left(\mathbf{v}\frac{\partial p}{\partial\eta}\right)d\eta. \tag{2.7}$$

3. An energy and angular-momentum conserving vertical finite-difference scheme

The vertical finite-difference scheme described in this section has elements in common with a number of schemes developed for the primitive equations. In particular it is a generalization of the sigma-coordinate scheme of Burridge and Haseler (1977), apart from a modification to the calculation of geopotential to ensure conservation of angular momentum.

a. Distribution of levels

Prognostic variables u, v and T (and more generally the moisture variable also) are carried, in general, at unequally-spaced, full levels $k = 1, 2, \ldots,$ NLEV, and we define values of the vertical coordinate $\eta_{k+1/2}$, and thus the pressure $p_{k+1/2}$ at intermediate half levels. The pressure difference between half levels is given by

$$\Delta p_k = p_{k+1/2} - p_{k-1/2}. \tag{3.1}$$

b. Continuity equation

The natural finite-difference analog of (2.6) is

$$\frac{\partial p_s}{\partial t} = -\sum_{r=1}^{\text{NLEV}} \nabla\cdot(\mathbf{v}_r\Delta p_r), \tag{3.2}$$

while (2.7) yields half-level values of $\dot{\eta}(\partial p/\partial\eta)$:

$$\left(\dot{\eta}\frac{\partial p}{\partial\eta}\right)_{k+1/2} = -\frac{\partial p_{k+1/2}}{\partial t} - \sum_{r=1}^{k} \nabla\cdot(\mathbf{v}_r\Delta p_r). \tag{3.3}$$

In evaluating (3.3) at time t, (3.2) should first be used to compute values of p_s at the following time step $t + \Delta t$. The new value of $p_{k+1/2}$ may then be calculated, and thus $\partial p_{k+1/2}/\partial t$ found using, for example, a centered difference in time. In the special case of sigma coordinates the rate of change of $p_{k+1/2}$ becomes simply

$$\frac{\partial p_{k+1/2}}{\partial t} = -\sigma_{k+1/2}\sum_{r=1}^{\text{NLEV}} \nabla\cdot(p_s\mathbf{v}_r)\Delta\sigma_r$$

and no such explicit time differencing is necessary.[1]

c. Vertical advection

Conservation of energy is preserved by the vertical advection terms if the advection of a variable F is such as to satisfy the finite-difference analogs of the relations

$$\int_0^1 \dot{\eta}\frac{\partial F}{\partial\eta}\frac{\partial p}{\partial\eta}\,d\eta = -\int_0^1 F\frac{\partial}{\partial\eta}\left(\dot{\eta}\frac{\partial p}{\partial\eta}\right)d\eta,$$

$$\int_0^1 \dot{\eta}F\frac{\partial F}{\partial\eta}\frac{\partial p}{\partial\eta}\,d\eta = -\int_0^1 \frac{1}{2}F^2\frac{\partial}{\partial\eta}\left(\dot{\eta}\frac{\partial p}{\partial\eta}\right)d\eta.$$

This is achieved by choosing

$$\left(\dot{\eta}\frac{\partial F}{\partial\eta}\right)_k = \frac{1}{2\Delta p_k}\left[\left(\dot{\eta}\frac{\partial p}{\partial\eta}\right)_{k+1/2}(F_{k+1} - F_k) + \left(\dot{\eta}\frac{\partial p}{\partial\eta}\right)_{k-1/2}(F_k - F_{k-1})\right]. \tag{3.4}$$

In the examples given in later sections this form is used for T as well as u and v. Arakawa and Lamb (1977) describe an alternative differencing for temperature in order to conserve $\ln\theta$, where θ is potential temperature.

d. The hydrostatic equation and pressure-gradient term

The form chosen for the finite-difference analog of the hydrostatic equation (2.4) is

[1] Such differencing may be avoided more generally by use of the relationship $\partial p/\partial t = (\partial p/\partial p_s)\partial p_s/\partial t$.

$$\phi_{k+1/2} - \phi_{k-1/2} = -RT_k \ln \frac{p_{k+1/2}}{p_{k-1/2}},$$

giving

$$\phi_{k+1/2} = \phi_s + \sum_{r=k+1}^{\text{NLEV}} RT_r \ln \frac{p_{r+1/2}}{p_{r-1/2}}, \quad (3.5)$$

where $\phi_{k+1/2}$ is a half-level value, ϕ_s the surface value, and we adopt the convention

$$\sum_{r=\text{NLEV}+1}^{\text{NLEV}} (\ ) \equiv 0.$$

When used in the momentum equations full-level values of ϕ are required and for the moment we write simply

$$\phi_k = \phi_{k+1/2} + \alpha_k RT_k. \quad (3.6)$$

It is not, in fact, necessary to specify α_k in order to ensure conservation of energy and angular momentum, and values may be chosen to enhance the accuracy of the scheme. A specific choice is made at the end of this subsection.

Intimately connected with the form chosen for the integration of the hydrostatic equation is the expression for full level values of the pressure gradient term $(RT/p)\nabla p$ in terms of the known half-level values $p_{k+1/2}$ and $\nabla p_{k+1/2}$. We determine this expression by requiring that the vertical difference scheme preserves the conservation of angular momentum:

$$\int_0^{2\pi} \left[\int_0^1 \left(\frac{\partial \phi}{\partial \lambda} + \frac{RT}{p} \frac{\partial p}{\partial \lambda} \right) \left(\frac{\partial p}{\partial \eta} \right) d\eta + \phi_s \frac{\partial p_s}{\partial \lambda} \right] d\lambda = 0,$$

where λ is longitude. This requires in finite-difference form,

$$\sum_{r=1}^{\text{NLEV}} \phi_r \frac{\partial}{\partial \lambda} \Delta p_r = \phi_s \frac{\partial p_s}{\partial \lambda} + \sum_{r=1}^{\text{NLEV}} R \left(\frac{T}{p} \frac{\partial p}{\partial \lambda} \right)_r \Delta p_r, \quad (3.7)$$

which is satisfied if

$$\left(\frac{RT}{p} \nabla p \right)_k = \frac{RT_k}{\Delta p_k} \left[\left(\ln \frac{p_{k+1/2}}{p_{k-1/2}} \right) \nabla p_{k-1/2} + \alpha_k \nabla (\Delta p_k) \right]. \quad (3.8)$$

Angular momentum conservation is hereby achieved without the artificial dependence of geopotential on the temperature of all model levels that occurs in the scheme described by Arakawa and Lamb (1977). This is a consequence of using half-level values of ϕ in the summation (3.5) of the hydrostatic equation.

The value of α_k in (3.6) and (3.8) must be specified in any application of the scheme outlined here. One choice could be to require cancellation of error in the sum of the geopotential and pressure gradient terms for a reference temperature distribution which is a function of pressure alone. Here we restrict attention to an alternative which causes (3.8) to reduce to the usual form

$$RT_k \nabla \ln p_s$$

for a sigma-coordinate model. This is achieved if

$$\alpha_k = 1 - \frac{p_{k-1/2}}{\Delta p_k} \ln \frac{p_{k+1/2}}{p_{k-1/2}}. \quad (3.9)$$

In this case (3.8) may be written

$$\left(\frac{RT}{p} \nabla p \right)_k = RT_k \nabla \left[\frac{1}{\Delta p_k} (p_{k+1/2} \ln p_{k+1/2} - p_{k-1/2} \ln p_{k-1/2}) \right]. \quad (3.10)$$

e. Energy-conversion term

To obtain a form for the term $\kappa T\omega/p$ in (2.2) we use (2.5) to write

$$\frac{\kappa T \omega}{p} = -\frac{\kappa T}{p} \int_0^\eta \nabla \cdot \left(\mathbf{v} \frac{\partial p}{\partial \eta} \right) d\eta + \kappa T \mathbf{v} \cdot \left(\frac{1}{p} \nabla p \right). \quad (3.11)$$

Full-level values of this expression are then determined by the requirement that the difference scheme conserves the total energy of the model atmosphere for adiabatic, frictionless motion. It may be confirmed that this is achieved by 1) evaluating the first term on the right-hand side of (3.11) at level k by

$$-\frac{\kappa T_k}{\Delta p_k} \left[\left(\ln \frac{p_{k+1/2}}{p_{k-1/2}} \right) \sum_{r=1}^{k-1} \nabla \cdot (\mathbf{v}_r \Delta p_r) + \alpha_k \nabla \cdot (\mathbf{v}_k \Delta p_k) \right], \quad (3.12)$$

and 2) evaluating the second term as

$$\kappa T_k \mathbf{v}_k \cdot \left(\frac{1}{p} \nabla p \right)_k, \quad (3.13)$$

where the term $(1/p\nabla p)_k$ is calculated in the same way as in the momentum equation.

f. The horizontal representation of the pressure gradient

In a model with a finite-difference representation in the horizontal, two alternative forms for the pressure gradient are suggested by equations (3.8) and (3.10). We illustrate these for a grid for which values of surface pressure (and thus pressure) and temperature are defined at the same point, and consider explicitly only the zonal derivative. We first define

the usual operators

$$\delta_\lambda A = [A(\lambda + \Delta\lambda/2) - A(\lambda - \Delta\lambda/2)]/\Delta\lambda,$$

$$\bar{A}^\lambda = \tfrac{1}{2}[A(\lambda + \Delta\lambda/2) + A(\lambda - \Delta\lambda/2)].$$

If the geopotential gradient is represented by

$$\frac{1}{a\cos\theta}\delta_\lambda\phi$$

where θ is latitude and a the radius of the earth, the appropriate form of the pressure gradient for conservation of angular momentum is derived from (3.8) and is

$$\frac{R}{a\cos\theta\overline{\Delta p_r}^\lambda}\left[\left(\overline{T_k \ln\frac{p_{k+1/2}}{p_{k-1/2}}}\right)^\lambda \delta_\lambda p_{k-1/2} + (\overline{\alpha_k T_k})^\lambda \delta_\lambda \Delta p_k\right], \quad (3.14)$$

provided the geopotential and pressure gradient terms are multiplied by $\overline{\Delta p_k}^\lambda$ in the expression for the rate of change of angular momentum.

An alternative representation of the pressure gradient term is derived directly from (3.10):

$$\frac{R\bar{T}^\lambda}{a\cos\theta}\delta_\lambda\left[\frac{1}{\Delta p_k}(p_{k+1/2}\ln p_{k+1/2} - p_{k-1/2}\ln p_{k-1/2})\right]. \quad (3.15)$$

This is direct generalization of the σ coordinate form

$$\frac{R\bar{T}^\lambda}{a\cos\theta}\delta_\lambda \ln p_s$$

discussed by Corby *et al.* (1972). For the present vertical scheme (3.15) implies exact cancellation of the geopotential and pressure gradient terms for a temperature profile of the form $T = A\ln p + B$ for finite $\Delta\lambda$ in the limit as $\Delta p_k \to 0$, and for finite Δp_k in a sigma coordinate model if full level pressures are appropriately defined, as discussed below.

Precise implementation of the vertical finite-difference scheme described above in a spectral model would require calculation of additional spectral/grid-point transforms associated with the computation of pressure gradients. However, for the continuous equations

$$\nabla p = \left(p_s\frac{\partial p}{\partial p_s}\right)_{\eta=\text{constant}}\nabla \ln p_s, \quad (3.16)$$

and if the definition $\eta = h(p, p_s)$ is used analytically to compute half-level values of $\partial p/\partial p_s$ as well as of p, we may use (3.16) to avoid additional transforms.

g. Full-level values of pressure

A feature of the finite-difference scheme described here is that no reference is made to full-level values of the vertical coordinate, or equivalently pressure. Such full-level values are required, however, for the determination of initial values of the prognostic variables u, v and T, and, more generally, as input to parameterization schemes.

Two different full-level values of p are suggested by the finite-difference scheme. (3.12) is an approximation to a term

$$-\frac{\kappa T}{p}\int_0^\eta \nabla\cdot\left(\mathbf{v}\frac{\partial p}{\partial\eta}\right)d\eta$$

and may generally be written

$$-\frac{\kappa T_k}{\Delta p_k}\ln\frac{p_{k+1/2}}{p_{k-1/2}}\left[\sum_{r=1}^{k-1}\nabla\cdot(\mathbf{v}_r\Delta p_r) + \left(\frac{1}{2} + O\left(\frac{\Delta p_k}{p_{k-1/2}}\right)\right)\nabla\cdot(\mathbf{v}_k\Delta p_k)\right].$$

For $k = 1$ the simplest equivalent is

$$-\frac{\kappa T_1}{(\Delta p_1/2)}[\tfrac{1}{2}\nabla\cdot(\mathbf{v}_1\Delta p_1)].$$

These expressions suggest the full-level values

$$\left.\begin{aligned} p_k &= \frac{\Delta p_k}{\ln(p_{k+1/2}/p_{k-1/2})}, \quad k > 1 \\ p_1 &= \tfrac{1}{2}\Delta p_1 \end{aligned}\right\}. \quad (3.17)$$

From (3.10) we obtain an alternative:

$$p_k = \exp\left[\frac{1}{\Delta p_k}(p_{k+1/2}\ln p_{k+1/2} - p_{k-1/2}\ln p_{k-1/2}) - C\right], \quad (3.18)$$

where C is independent of the horizontal coordinates. Setting $C = 1$ yields an appropriate p_k in the limit $\Delta p_k/p_{k-1/2} \to 0$ and also a full-level value for p_1 which is consistent with the hydrostatic equation [see (3.6) and (3.9)] for an isothermal upper atmosphere.

Away from the upper boundary (3.17) and (3.18) both yield

$$p_k = \tfrac{1}{2}(p_{k+1/2} + p_{k-1/2}) + O[(\Delta p_k)^2/p_{k-1/2}],$$

but top-level values are given by $\Delta p_1/2$ and $\Delta p_1/e$, respectively. This ambiguity may be resolved at the possible expense of angular momentum conservation by using the value $\alpha_1 = \ln 2$ in (3.6) and (3.12). In this case

$$\phi_1 = \phi_{1\,1/2} + (\ln 2)RT_1 \quad (3.19)$$

and C in (3.18) should take the value 1 at all but the top level where $C = \ln 2$. Loss of angular momentum conservation will not occur if the uppermost coordinate surfaces are surfaces of constant pressure.

We return to this point with specific examples in later sections.

4. Gravity waves and a semi-implicit time scheme

We here follow the development given for a sigma-coordinate model by Hoskins and Simmons (1975). For the more general vertical coordinate it is necessary to introduce not only a reference temperature profile, but also a reference value for the surface pressure. Variables defined at each of the NLEV levels of the model are represented by column vectors, and we denote the reference temperature profile by $\mathbf{T}_r$ and the reference pressure by p_r.

Linearizing about the resting basic state $(\mathbf{T}_r, p_r)$.[2] the divergence, temperature, surface pressure and hydrostatic equations may be written

$$\frac{\partial \mathbf{D}}{\partial t} = \underset{\sim}{\mathscr{D}} - \nabla^2(\boldsymbol{\phi} + \mathbf{h}_1 p_s'), \tag{4.1}$$

$$\frac{\partial \mathbf{T}'}{\partial t} = \underset{\sim}{\mathscr{T}} - \underset{\sim}{\tau}\mathbf{D}. \tag{4.2}$$

$$\frac{\partial p_s'}{\partial t} = \mathscr{P} - \boldsymbol{\nu}\cdot\mathbf{D}, \tag{4.3}$$

$$\boldsymbol{\phi} = \underset{\sim}{\mathscr{H}} + \underset{\sim}{\gamma}\mathbf{T}' + \mathbf{h}_2 p_s'. \tag{4.4}$$

Here $\mathbf{D}$ is the divergence, $\mathbf{T}' = \mathbf{T} - \mathbf{T}_r$, $p_s' = p_s - p_r$, and $\underset{\sim}{\mathscr{D}}$, $\underset{\sim}{\mathscr{T}}$, $\mathscr{P}$ and $\underset{\sim}{\mathscr{H}}$ contain all nonlinear terms. The constant matrices and vectors $\underset{\sim}{\gamma}$, $\underset{\sim}{\tau}$, $\mathbf{h}_1$, $\mathbf{h}_2$ and $\boldsymbol{\nu}$ are defined in the Appendix for the vertical scheme described in the preceding section.

Neglecting the nonlinear terms leads to the gravity-wave equation

$$\frac{\partial^2 \mathbf{D}}{\partial t^2} = \nabla^2 \underset{\sim}{\mathbf{B}}\mathbf{D},$$

where

$$\underset{\sim}{\mathbf{B}} = \underset{\sim}{\gamma}\underset{\sim}{\tau} + (\mathbf{h}_1 + \mathbf{h}_2)\cdot\boldsymbol{\nu} \tag{4.5}$$

The eigenvalues of $\underset{\sim}{\mathbf{B}}$ are the squares of the gravity-wave phase speeds, and examples are presented in Section 7.

Eqs. (4.1) to (4.4) may readily be used to define a semi-implicit time scheme. Just as in a sigma-coordinate model, the nonlinear terms $\underset{\sim}{\mathscr{D}}$, $\underset{\sim}{\mathscr{T}}$, $\mathscr{P}$ and $\underset{\sim}{\mathscr{H}}$ are evaluated at time t, while the linear terms on the right-hand sides are evaluated as the arithmetic mean of values at time $t + \Delta t$ and $t - \Delta t$. The largest difference from a sigma-coordinate scheme is the more complicated form of the hydrostatic equation, which includes a term to be evaluated explicitly.

Simmons *et al.* (1978) demonstrated that the reference temperature profile $\mathbf{T}_r$ must be carefully chosen to avoid computational instability in a sigma coordinate model. More generally, similar considerations apply to the choice of the reference surface pressure. Specific examples are discussed in Section 7.

5. The vertical coordinates

As mentioned in the Introduction, we examine the performance of the difference schemes outlined in preceding sections for three vertical coordinates. The first is the usual sigma coordinate (Phillips, 1957) for which

$$p_{k+1/2} = p_s\eta_{k+1/2} \quad \text{and} \quad (\partial p/\partial p_s)_{k+1/2} = \eta_{k+1/2}.$$

The second is in essence the hybrid coordinate described by Arakawa and Lamb (1977). For this coordinate we define an inter-facial pressure $p_{I+1/2}$ with corresponding half-level value $\eta_{I+1/2}$. Then

$$p_{k+1/2} = p_{I+1/2}\eta_{k+1/2}/\eta_{I+1/2} \quad \text{for} \quad \eta_{k+1/2} \leqslant \eta_{I+1/2}$$

and

$$p_{k+1/2} = p_{I+1/2} + (\eta_{k+1/2} - \eta_{I+1/2})(p_s - p_{I+1/2})/(1 - \eta_{I+1/2}) \quad \text{otherwise,}$$

with

$$\left(\frac{\partial p}{\partial p_s}\right)_{k+1/2} = 0 \quad \text{for} \quad \eta_{k+1/2} \leqslant \eta_{I+1/2},$$

$$= (\eta_{k+1/2} - \eta_{I+1/2})/(1 - \eta_{I+1/2}) \quad \text{otherwise.}$$

The third vertical coordinate is designed to have smoothly varying layer thicknesses, but to tend to a pressure coordinate at upper levels. In continuous form we define

$$\eta = \frac{p}{p_s} + \left(\frac{p}{p_s} - 1\right)\left(\frac{p}{p_s} - \frac{p}{p_0}\right), \quad p_0 \text{ a constant.}$$

Then $\eta = 1$ when $p = p_s$ and $\eta \sim p/p_0$ as $p \to 0$. η varies monotonically from $p = p_s$ to $p = 0$ provided $p_0 > \frac{1}{2}\,\mathrm{Max}(p_s)$. In the following examples we choose $p_0 = 1013.2$ mb. In this case the pressure on a coordinate surface varies by about 1% near the 10 mb level as the surface pressure varies in the range 1013 mb $> p_s >$ 500 mb.

We refer to this third vertical coordinate as the modified hybrid coordinate. Half-level values are given by

$$p_{k+1/2} = \frac{2p_0\eta_{k+1/2}}{[1 + (1 + 4\eta_{k+1/2}p_0(p_0 - p_s)/p_s^2)^{1/2}]},$$

$$\left(\frac{\partial p}{\partial p_s}\right)_{k+1/2} = \frac{p_{k+1/2}(p_{k+1/2}/p_s)^2(2p_0/p_s - 1)}{(2\eta_{k+1/2}p_0 - p_{k+1/2})}.$$

In subsequent sections we present a sample of results of idealized tests of the different coordinates and finite-difference scheme. For illustrative purposes attention is concentrated on one particular distribution of unequally-spaced vertical levels, although comparisons have been made with lower and

[2] Linearization about $\ln p_r$ rather than p_r is found to result in a less stable scheme for hybrid coordinates.

higher resolution results obtained using an equal layer spacing.

The unequal distribution of levels is that used for operational forecasting with a sigma-coordinate model at ECMWF. 15 full levels are used and half-level values of η are given by

$$\eta_{k+1/2} = 0.75s_k + 1.75s_k^3 - 1.5s_k^4,$$
$$s_k = k/\text{NLEV}. \quad (5.1)$$

Values of $p_{l+1/2}$ for the hybrid model are chosen such that half-level pressures are identical to those of the sigma and modified hybrid models for a surface pressure of 1013.2 mb. Computations are performed for the interface at $\eta_{2\ 1/2}$ and $\eta_{4\ 1/2}$, that is at pressures of 105 and 229 mb, respectively. Thus layer thicknesses vary smoothly for the surface pressure of 1013.2 mb, but exhibit an abrupt variation for surface pressures representative of those occurring over high ground.

Half-level pressures are given in Table 1, together with alternative values for full-level pressures. (a) and (b) refer to results calculated according to (3.17) and (3.18) (with $C = 1$), (c) gives the arithmetic mean of full-level values, while (d) gives results calculated from full-level values η_k computed from the same formula as (5.1) but with $s_k = (k - \frac{1}{2})/\text{NLEV}$.

The alternative full-level pressures are evidently very similar away from the upper and lower boundaries, the values (b) lying between those of (a), (c) and (d), while top-level differences are as anticipated in Section 3g. The rapid variation in layer thicknesses at low levels, chosen for the parameterization of boundary-layer processes, results in the difference between the bottom full-level pressure and the surface pressure being a factor of two different when calculated from (5.1) as compared with the value implied by the finite-difference scheme. This difference should be noted when parameterization schemes are designed.

In the following explicit examples we adopt expression (3.18) with $C = 1$ at all but the top level, where we take $p_1 = \frac{1}{2}\Delta p_1$. Tests indicate that results are generally insensitive to this choice.

6. Cancellation of geopotential and pressure gradient terms over steep orography

Reference has been made in the introduction to a number of authors who have examined the error in the representation of the pressure gradient over steep orography, and we repeat such calculations here in order to compare the hybrid and sigma coordinates.

We consider a temperature field which is a function of pressure alone. In the continuous formulation the last two terms on the left-hand side of (2.1) cancel exactly. Noting that

TABLE 1. Half-level and alternative full-level values of pressure for a 15-level vertical resolution with a surface pressure of 1013 mb.

		p_k (mb)			
k	$p_{k+1/2}$ (mb)	(a)	(b)	(c)	(d)
1	51	26	19	26	25
2	105	75	77	78	78
3	164	132	133	134	134
4	229	194	195	196	195
5	300	263	264	264	264
6	379	338	339	339	339
7	463	419	420	421	420
8	551	506	506	507	507
9	642	595	596	597	597
10	732	686	686	687	687
11	817	774	774	774	775
12	893	855	855	855	857
13	955	924	924	924	926
14	998	976	976	976	979
15	1013	1005	1005	1005	1009

$$\nabla\phi_s = -\frac{RT(p_s)}{p_s}\nabla p_s,$$

the corresponding finite-difference value of the sum of the two terms may be written

$$\begin{aligned} E_k(p_s)\nabla p_s = &-\frac{RT(p_s)}{p_s}\nabla p_s + \alpha_k R\nabla T_k \\ &+ RT_k\left(\frac{\partial\alpha_k}{\partial p_s}\right)\nabla p_s + \sum_{j=k+1}^{\text{NLEV}} R\left\{(\nabla T_j)\ln\frac{p_{j+1/2}}{p_{j-1/2}}\right. \\ &\left. + T_j\left[\frac{1}{p_{j+1/2}}\left(\frac{\partial p}{\partial p_s}\right)_{j+1/2} - \frac{1}{p_{j-1/2}}\left(\frac{\partial p}{\partial p_s}\right)_{j-1/2}\right]\nabla p_s\right\} \\ &+ \frac{RT_k}{\Delta p_k}\left\{\left(\ln\frac{p_{k+1/2}}{p_{k-1/2}}\right)\left(\frac{\partial p}{\partial p_s}\right)_{k-1/2}\right. \\ &\left. + \alpha_k\left[\left(\frac{\partial p}{\partial p_s}\right)_{k+1/2} - \left(\frac{\partial p}{\partial p_s}\right)_{k-1/2}\right]\right\}\nabla p_s, \quad (6.1) \end{aligned}$$

where

$$\nabla T_k = \left(\frac{dT}{dp}\right)_{p=p_k}\left(\frac{\partial p_k}{\partial p_s}\right)\nabla p_s.$$

In evaluating these expressions we calculate $\partial\alpha_k/\partial p_s$ and $\partial p_k/\partial p_s$ from values of $(\partial p/\partial p_s)_{k-1/2}$ and $(\partial p/\partial p_s)_{k+1/2}$ using (3.9) and (3.17) or (3.18).

The error function $E_k(p_s)$ has been calculated for a number of temperature profiles, and we illustrate results for the profile shown in Fig. 1. This profile comprises two segments in which the temperature depends linearly on $\ln p$. The relatively sharp tropopause results in the possibility of significant stratospheric error, for reasons discussed by Sundqvist (1976).

Plots of the error are presented in Fig. 2 for the 15-level resolution specified in the preceding section

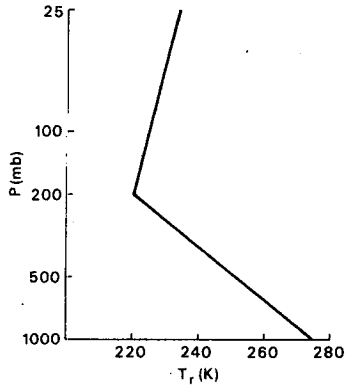

FIG. 1. A reference vertical profile of temperature.

with $p_s = 1013.2$ mb and $p_s = 750$ mb, respectively. For display purposes this error is expressed dimensionally as a geostrophic wind error assuming $f = 10^{-4}$ s^{-1} and a large, though not unrealistic surface pressure change of 10% over 100 km.

In all cases the tropospheric error is low for this vertical finite-difference scheme. In particular it vanishes identically for the sigma-coordinate case. It is a matter of simple algebra to demonstrate that choosing definition (3.18), with $C = 1$, the pressure-gradient error vanishes identically for a temperature profile $A \ln p + B$. A similar result for a different finite-difference scheme has been presented by Corby *et al.* (1972).

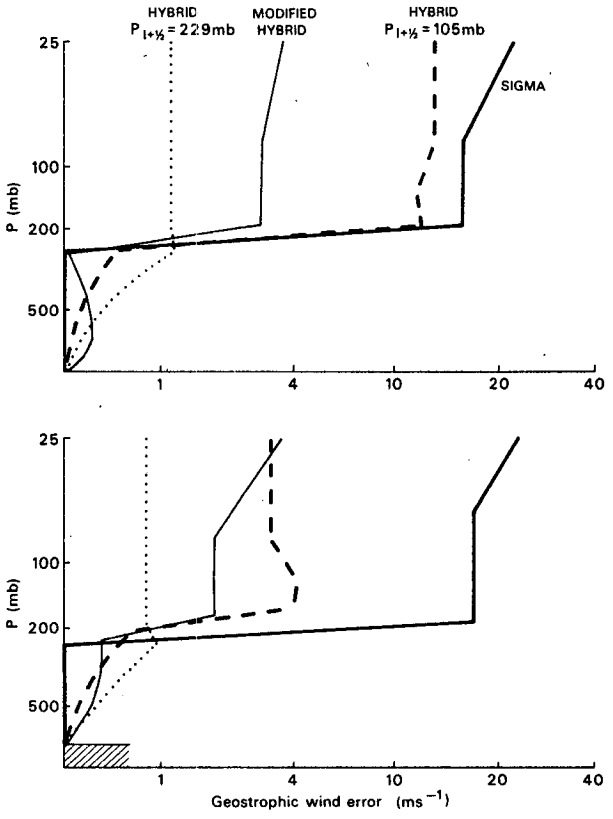

FIG. 2. The variation with height of the geostrophic wind error associated with error in the representation of the geopotential and pressure gradients. The heavy solid curve is that for the sigma coordinate, the light solid curve that for the modified hybrid coordinate, the dashed curve the hybrid model with $p_{I+1/2} = 105$ mb and the dotted curve the corresponding calculation with $p_{I+1/2} = 229$ mb.

TABLE 2. Phase speeds of the lowest five gravity-wave modes for two values of the surface pressure. Coordinate type 1 is the sigma coordinate, types 2 and 3 are the hybrid coordinate with $p_{I+1/2} = 105$ and 229 mb, respectively, and type 4 is the modified hybrid coordinate.

p_s (mb)	Coordinate type 1	2	3	4
1013.2	309	309	309	309
	183	183	183	183
	82	82	82	82
	48	48	48	48
	30	30	30	30
500	303	302	301	302
	185	166	166	169
	94	71	71	75
	51	36	34	38
	32	24	21	25

In contrast, substantial variations are found in the error above the tropopause. It is particularly large for the sigma coordinate, and generally smaller for the hybrid coordinate with $p_{I+1/2} = 105$ mb, and for the modified hybrid coordinate. A consequence of the form of the hybrid coordinate is that the error is independent of height above the interface, and we thus find particularly small stratospheric errors when the interface is located at the tropospheric pressure $p_{I+1/2} = 229$ mb, although errors below this level are larger. Some other disadvantages of such a choice are discussed in the following section.

For the sigma-coordinate case the stratospheric error is independent of pressure at all but the top level. This is again a consequence of the logarithmic temperature profile. The increase in the error at the topmost level is due to the choice $p_1 = \frac{1}{2}\Delta p_1$, rather than the form (3.18) with $C = 1$. However, it may be removed by adopting the modification (3.19) to the calculation of the topmost geopotential.

7. The stability of the semi-implicit time scheme

Phase speeds of the lowest five gravity-wave modes, computed as outlined in Section 4, are presented in Table 2 for two different surface pressures and for the four cases discussed in the preceding section. Phase speeds are found to be almost identical for the surface pressure of 1013.2 mb, for which half-level pressures are identical, but significant differences are seen for the surface pressure of 500 mb, larger differences between speeds for the two surface pressures being found for the hybrid coordi-

nates. This suggests that the semi-implicit time scheme may be less stable for hybrid coordinate systems.

We have thus examined the stability of the generalized semi-implicit scheme described in Section 4 precisely as carried out for a sigma-coordinate scheme by Simmons *et al.* (1978). In each case stability was examined for time steps varying from 5–60 min in increments of 5 min, assuming a length scale equivalent to the smallest retained scale in a spectral model with triangular truncation at wavenumber 63.

Results are summarized in Table 3 for the temperature profile shown in Fig. 1. The modified hybrid coordinate scheme is apparently little more unstable than the sigma-coordinate scheme, but the instability becomes more marked for the hybrid coordinate. This is particularly the case when the interface is located in the upper troposphere.

The instability suggested by Table 3 has been found in practice. The semi-implicit grid-point model used operationally at ECMWF has been modified to include the hybrid vertical coordinates and difference schemes described here. Test integrations have been performed using the 15-level vertical resolution illustrated in Table 1, and a horizontal resolution of 3.75° for the regular latitude-longitude grid. A dry-adiabatic convective adjustment, surface friction and a linear, biharmonic horizontal diffusion of momentum and temperature were included. An initial analysis for 16 January 1979 was used.

Integrations with a time step of 30 min and a reference surface pressure of 1013.2 mb were found to become unstable over the Himalayas after about 3.5 days for the interfacial pressure of 229 mb. They were, however, completed successfully up to 7 days by changing the reference surface pressure to 800 mb. Successful 7-day integrations were completed with a 1013.2 mb reference pressure in all other cases.

Examining the stability of the semi-implicit scheme for a tropospheric lapse rate larger than shown in Fig. 1 reveals a further possible problem for the hybrid coordinate in that an unstable gravity-wave mode was found for a surface pressure of 500 mb when the interface was located in the troposphere, whereas all modes were stable for a stratospheric interface, and also when calculated using the sigma and modified hybrid coordinates. This may be readily understood by examining the form (3.4) chosen for the vertical advection terms to ensure conservation. If the vertical velocity, $\dot{\eta}\partial p/\partial\eta$, varies slowly with pressure the finite-difference approximation to $\partial T/\partial p$ at level k is

$$\frac{1}{2\Delta p_k}(T_{k+1} - T_{k-1}).$$

If Γ is the actual gradient at level k this finite-difference form may be written approximately as

TABLE 3. The stability of the semi-implicit scheme. *S* denotes stability for all time steps examined, while unstable cases are denoted by the smallest time step for which instability is found. Coordinate types are as in Table 2.

p_s (mb)	p_r (mb)	Coordinate type 1	2	3	4
1013.2	1013.2	*S*	*S*	*S*	*S*
750	1013.2	*S*	*S*	*S*	*S*
500	1013.2	*S*	*S*	35	*S*
1013.2	750	*S*	45	50	*S*
750	750	*S*	*S*	*S*	*S*
500	750	*S*	*S*	45	*S*
1013.2	500	5	5	5	5
750	500	*S*	25	5	60
500	500	*S*	*S*	*S*	*S*

$$\frac{p_{k+1} - p_{k-1}}{2\Delta p_k}\Gamma \approx \left[\frac{1}{2} + \frac{1}{4}\left(\frac{\Delta p_{k-1} + \Delta p_{k+1}}{\Delta p_k}\right)\right]\Gamma.$$

This evidently yields a good approximation to Γ if the layer thicknesses vary smoothly, but over the highest mountains thicknesses may vary by a factor of more than two across the interface. The temperature gradient may thus be overestimated by at least 25% immediately below the interface, and this can lead to gravitational instability if the interface is located in the troposphere. Immediately above the interface the gradient is underestimated by a similar amount.

8. Concluding remarks

We have introduced an energy and angular momentum conserving vertical finite-difference scheme for a general terrain-following vertical coordinate which is a function of pressure and its surface value. For an appropriate definition of full-level pressure the error in the pressure gradient over steep orography vanishes for a logarithmic temperature profile in the special case of sigma coordinates. The formulation of the finite-difference scheme is such that a change of vertical coordinate requires only a change in the calculation of half-level values of pressure and the constant matrices and vectors of the semi-implicit scheme. The computational cost of including this flexibility in a model is unlikely to be large.

Estimates of the error in the pressure gradient over steep orography indicate generally small tropospheric values, but large sigma-coordinate errors above a sharp tropopause. These errors are partially reduced for the hybrid vertical coordinate when the interface above which the coordinate reduces to pressure is located in the stratosphere, and substantially reduced when the interface is located just below the tropopause. In the latter case, however, the semi-implicit time scheme is less stable over high orography, and a spurious gravitational instability may occur below the interface. A compromise between computational stability and the ac-

curacy of the stratospheric pressure gradient may be found with the modified hybrid coordinate introduced in Section 5.

It is not within the scope of this paper to make specific recommendations concerning the choice of vertical coordinate. In practice the best choice will very much depend on the purpose for which the primitive equation model is to be used, the vertical resolution that can be employed, and the type of orography used. Studies such as that reported here may help guide this choice. Regarding the specific field of numerical weather prediction it is our intention to compare in a future paper medium-range forecasts performed using the vertical coordinates and difference scheme discussed here.

Note added in proof. Alternative coordinates may also be used. Successful tests have recently been carried out using several coordinates of the form $p_{k+1/2} = A_{k+1/2}p_j + B_{k+1/2}p_s$, where the A's and B's vary only with the vertical level.

APPENDIX

Matrices and Vectors for the Semi-Implicit Scheme

In order to linearize (4.1)–(4.4) it is necessary to specify half-level values of $\partial p/\partial p_s$ as well as p. The matrices and vectors introduced in section 4 are then given by

$$(\underset{\sim}{\gamma})_{jk} = \begin{cases} 0, & k < j \\ R\alpha_k, & k = j \\ R \ln \dfrac{p_{k+1/2}}{p_{k-1/2}}, & k > j \end{cases}$$

$$(\underset{\sim}{\tau})_{jk} = \frac{\Delta p_k}{\Delta p_j}\kappa T_{rj}(\underset{\sim}{\gamma})_{kj} + \frac{1}{2\Delta p_j} \times \left\{(T_{r(j+1)} - T_{rj})\left[\left(\frac{\partial p}{\partial p_s}\right)_{j+1/2}\Delta p_k - \begin{vmatrix} 0, & k > j, \\ \Delta p_k, & k \leq j, \end{vmatrix}\right] + (T_{rj} - T_{r(j-1)}) \times \left[\left(\frac{\partial p}{\partial p_s}\right)_{j-1/2}\Delta p_k - \begin{vmatrix} 0, & (k+1) > j, \\ \Delta p_k, & (k+1) \leq j, \end{vmatrix}\right]\right\}$$

$$(\nu)_j = \Delta p_j$$

$$(\mathbf{h}_1)_j = \frac{RT_{rj}}{\Delta p_j}\left\{\left(\ln \frac{p_{j+1/2}}{p_{j-1/2}}\right)\left(\frac{\partial p}{\partial p_s}\right)_{j-1/2} + \alpha_j\left[\left(\frac{\partial p}{\partial p_s}\right)_{j+1/2} - \left(\frac{\partial p}{\partial p_s}\right)_{j-1/2}\right]\right\}$$

$$(\mathbf{h}_2)_j = RT_{rj}\frac{\partial \alpha_j}{\partial p_s} + \sum_{k=j+1}^{\text{NLEV}} RT_{rk}\left\{\frac{1}{p_{k+1/2}}\left(\frac{\partial p}{\partial p_s}\right)_{k+1/2} - \frac{1}{p_{k-1/2}}\left(\frac{\partial p}{\partial p_s}\right)_{k-1/2}\right\}.$$

If

$$\alpha_j = 1 - \frac{p_{j-1/2}}{\Delta p_j}\ln\frac{p_{j+1/2}}{p_{j-1/2}},$$

then $\partial\alpha_j/\partial p_s$ may readily be expressed as a function of $(\partial p/\partial p_s)_{j-1/2}$ and $(\partial p/\partial p_s)_{j+1/2}$. In this case we find

$$(\mathbf{h}_1 + \mathbf{h}_2)_j = \frac{RT_{rj}}{p_{j+1/2}}\left(\frac{\partial p}{\partial p_s}\right)_{j+1/2} + \sum_{k=j+1}^{\text{NLEV}} RT_{rk} \times \left\{\frac{1}{p_{k+1/2}}\left(\frac{\partial p}{\partial p_s}\right)_{k+1/2} - \frac{1}{p_{k-1/2}}\left(\frac{\partial p}{\partial p_s}\right)_{k-1/2}\right\}.$$

All expressions are evaluated at the reference surface pressure p_r.

REFERENCES

Arakawa, A., and V. R. Lamb, 1977: Computational design of the basic dynamical processes of the UCLA general circulation model. *Methods in Computational Physics*, Vol. 17, J. Chang, Ed., Academic Press, 337 pp.

Burridge, D. M., and J. Haseler, 1977: A model for medium range weather forecasting—Adiabatic formulation. ECMWF Tech. Rep. No. 4, 46 pp.

Corby, G. A., A. Gilchrist and R. L. Newson, 1972: A general circulation model of the atmosphere suitable for long period integration. *Quart. J. Roy. Meteor. Soc.*, **98**, 809–832.

Fels, S. B., J. D. Mahlman, M. D. Schwarzkopf and R. W. Sinclair, 1980: Stratospheric sensitivity to perturbations in ozone and carbon dioxide: Radiative and dynamical response. *J. Atmos. Sci.*, **37**, 2265–2297.

Gary, J. M., 1973: Estimate of truncation error in transformed coordinate, primitive equation atmospheric models. *J. Atmos. Sci.*, **30**, 223–233.

Hoskins, B. J., and A. J. Simmons, 1975: A multi-layer spectral model and the semi-implicit method. *Quart. J. Roy. Meteor. Soc.*, **101**, 637–655.

Kasahara, A., 1974: Various vertical coordinate systems used for numerical weather prediction. *Mon. Wea. Rev.*, **102**, 509–522.

Nakamura, H., 1978: Dynamical effects of mountains on the general circulation of the atmosphere: I. Development of finite-difference schemes suitable for incorporating mountains. *J. Meteor. Soc. Japan*, **56**, 317–339.

Phillips, N. A., 1957: A coordinate system having some special advantages for numerical forecasting. *J. Meteor.*, **14**, 184–185.

Sangster, W. E., 1960: A method of representing the horizontal pressure force without reduction of station pressures to sea level. *J. Meteor.*, **17**, 166–176.

Schlesinger, M. E., and Y. Mintz, 1979: Numerical simulation of ozone production, transport and distribution with a global atmospheric general circulation model. *J. Atmos. Sci.*, **36**, 1325–1361.

Simmons, A. J., B. J. Hoskins and D. M. Burridge, 1978: Stability of the semi-implicit time scheme. *Mon. Wea. Rev.*, **106**, 405–412.

Sundqvist, H., 1976: On vertical interpolation and truncation in connexion with use of sigma system models. *Atmosphere*, **14**, 37–52.